LAWRENCE
LIVERMORE
NATIONAL
LABORATORY

UCRL-TR-213455

Optimization of Focusing by Strip and Pixel Arrays

G. J. Burke, D. A. White, C. A. Thompson

July 8, 2005

This work was performed under the auspices of the U.S. Department of Energy by University of California, Lawrence Livermore National Laboratory under Contract W-7405-Eng-48.

Optimization of Focusing by Strip and Pixel Arrays *

G. J. Burke, D. A. White, C. A. Thompson
Lawrence Livermore National Laboratory, Livermore, CA 94550

Introduction

Professor Kevin Webb and students at Purdue University have demonstrated the design of conducting strip and pixel arrays for focusing electromagnetic waves [1, 2]. Their key point was to design structures to focus waves in the near field using full wave modeling and optimization methods for design. Their designs included arrays of conducting strips optimized with a downhill search algorithm and arrays of conducting and dielectric pixels optimized with the iterative direct binary search method. They used a finite element code for modeling.

This report documents our attempts to duplicate and verify their results. We have modeled 2D conducting strips and both conducting and dielectric pixel arrays with moment method and FDTD codes to compare with Webb's results. New designs for strip arrays were developed with optimization by the downhill simplex method with simulated annealing. Strip arrays were optimized to focus an incident plane wave at a point or at two separated points and to switch between focusing points with a change in frequency. We also tried putting a line current source at the focus point for the plane wave to see how it would work as a directive antenna. We have not tried optimizing the conducting or dielectric pixel arrays, but modeled the structures designed by Webb with the moment method and FDTD to compare with the Purdue results.

Results

Strip Arrays

In [1] by K. R. Webb and students a figure is included that shows the focusing of a plane wave by an array of conducting strips. The strips are grouped into eight layers with parameters optimized to focus the wave below the array at two points separated by 4λ. The array was designed by optimization, where the variable parameters for strips in each layer were the initial offset, period, duty cycle (strip to period length ratio) and number of strips.

We have attempted to reproduce these results with a moment method code for conducting strips. Since the strip parameters were not given in [1] we first attempted to measure them from the figure. Later Webb and Li sent the actual parameters used [3], which differed slightly from our measured values. The strip arrays for both sets of parameters are plotted in Fig. 1. The moment method solution for downward Poynting's vector P_y over the region of the array for parameters measured from Webb's plot is shown in Fig. 2. The plane wave was incident from above with $P_y = 1$. Although there is considerable shadowing by the strips, some focusing can be seen at the indicated points. The results for P_y using the parameters from [3] are shown in Fig. 3. This model shows less focusing than with the

* This work was performed under the auspices of the U. S. Department of Energy by the University of California, Lawrence Livermore National Laboratory under Contract No. W-7405-Eng-48.

measured parameters. One reason for this difference may be that Webb designed the arrays with strips having a thickness of 0.1λ while our strips have zero thickness. We next used the parameters measured from Webb's plot and re-optimized using the downhill simplex method with simulated annealing [4]. Parameters optimized were the layer offset, period, duty cycle and layer spacing, the latter being the same for all layers. This re-optimized array is shown in Fig. 4 with the array measured from the figure in [1] for comparison. The pattern for P_y in Fig. 5 shows enhanced focusing at the points $x = -.06$ and 0.06 m which are about 4λ apart for the scale here of 10 GHz. This re-optimized array was also modeled with a 2D FDTD code. Results for E_z and P_y in Fig. 6 and 7 show good agreement between the moment method and FDTD solutions.

We next tried optimizing an array from scratch, using eight layers and optimizing the number of strips in each layer, the period length, duty cycle and inter-layer spacing. To start the optimization, each layer had 11 strips with initial strip edge at $x = -3.5$ cm and final strip edge at $x = +3.5$ cm. The duty cycles, starting at the bottom, were 0.4 for layers 1 and 2, 0.3 for layers 3 and 4, 0.2 for layers 5 and 6 and 0.1 for layers 7 and 8. An initial optimized array was obtained, shown in Fig. 8 as red lines. The solutions for E_z and P_y for this initial design, in Fig. 9, show focusing at $x = -0.06$ and 0.06 m but with unequal peaks. The initial result was saved and read into the optimization program again to randomize the simplex in a narrower range. After further optimization with simulated annealing the green array in Fig. 8 was obtained that produced more equal focusing, as shown in Fig. 10. It was found in other cases also that sometimes simulated annealing could improve a design, but sometimes it was better to generate a new randomized simplex centered on the current best case. A strip array optimized to focus at $y = -0.03$ m at 10 GHz, which is one wavelength below the lower strips, is shown in Fig. 11.

A design for focusing at a single point at $x = 0$, $y = -0.06$ m is shown in Fig. 12, with the resulting distributions of E_z and P_y plotted in Fig. 13. The strip parameters for generating the initial simplex were the same as for Fig. 8. Stronger fields are obtained at the single focus than when the focus is split. An array designed to focus at $x = -.06$ m at 9.5 GHz and $x = 0.06$ m at 10 GHz is shown in Fig. 14 and the distributions of P_y in Fig. 15.

From reciprocity it would be expected that placing a line current source at the position where the plane wave was focused should result in radiation directed back toward the incident plane wave source. A result of doing this experiment with the strip array in Fig. 12 is shown in Fig. 16 and 17. Focusing of the line source field is evident around 90° in the upward direction, but there is considerable reflection downward from the strip array. To reduce the backward radiation, the strip array can be put in a box. A result for a strip array in a rectangular box is shown in Fig. 18 and 19. The strips were optimized to focus an incident plane wave at $x = 0$, $y = -0.06$ m in the box, and a line source was then located at the focus point to evaluate the radiated field. The solution for an incident plane wave showed a large cavity mode in the lower part of the box, and that is also evident for the transmitting case in Fig. 18. The radiation pattern in Fig. 19 shows a weak maximum around 90°, but the pattern is degraded by the cavity modes. Multiple optimization attempts in the rectangular box resulted in similar solutions.

To disrupt the cavity modes the strip array was optimized in a box with an angled bottom, as shown in Fig. 20. Fig. 20(a) is a result of optimizing for a plane wave to focus at

$x = 0$, $y = -0.06$ m, while Fig. 20(b) was a result of optimizing the upward radiated field for a line current source at $x = 0$, $y = -0.06$ m. Since these are reciprocal configurations, the difference is considered a result of chance. The near E_z field and Poynting's vector P_y for the antennas of Fig. 20(a) and 20(b) are shown in Fig. 21 and 22, respectively. A strong cavity mode is still seen in the box, although it cannot be compared directly with the rectangular box since the plot ranges were not the same. The field and Poynting's vector in the angled box without the strip array is shown in Fig. 23. The radiation patterns for the antennas of Fig. 20(a) and 20(b) are compared in Fig. 24 with the pattern of the source in the open box. The strips are seen to enhance the directivity of the open horn antenna, although in all cases the illumination of the aperture is far from uniform, and the gain is less than could be achieved with a well designed horn.

Conducting Pixel Arrays

A result is also included in [1] showing focusing by an array of conducting pixels designed so that the focus point shifts from right to left with frequency. Webb and Li used the iterative direct binary search method to optimize the pixel locations. It appears that there has been a considerable amount of work on this method done at Purdue for optimizing pixels in printing graphics. We have not tried repeating the optimization, but did try modeling the structure shown in [1] with the moment method and FDTD. A comparison of the figure from [1] with the moment method result is shown in Fig. 25 for the reference frequency $\lambda = \lambda_0$. The structure is designed for a plane wave incident from 30° to the right of vertical. Good agreement is seen between the moment method and the finite element solution in [1]. A comparison is shown in Fig. 26 for $\lambda = 1.1\lambda_0$, where the array is designed to focus to the right, and again good agreement is obtained with Webb's results. The outside boundaries of the pixels were modeled with four strips per side in the moment method code.

The moment method solution is compared with FDTD in Fig. 27 for $\lambda = \lambda_0$. This appeared to be a difficult frequency, but the FDTD solution is converging toward the moment method solution. The FDTD result for $\lambda = 1.1\lambda_0$ is shown in Fig. 28 and is in good agreement with the moment method and the result from [1] reproduced in Fig. 26. Moment method solutions for λ/λ_0 from 0.98 to 1.05, in Fig. 29, show that the focusing is cutting off around $\lambda/\lambda_0 = 1$, which may account for the sensitivity of the FDTD solution there.

Dielectric Pixel Arrays

Webb and Li also optimized arrays of dielectric pixels by the iterative direct binary search method [1, 2]. To compare with these results we used a moment method solution of the volume dielectric integral equation [5] and FDTD. The moment method code was tested on a dielectric lens with the results shown in Fig. 30. The results look reasonable, with increased field around the optical focus of the lens which is marked on the plots.

Two pixel array designs are included in [1]. Fig. 5 in [1], reproduced here as Fig. 31, is for a background medium of silicon ($\epsilon_r = 12.1104$) with pixels of silicon dioxide ($\epsilon_r = 2.0852$) at $\lambda = 1.55$ μm. The plot scales are normalized to the wavelength in silicon at the reference frequency (λ_{Si}) and the pixels are $0.2\lambda_{\mathrm{Si}}$ on a side. The array is designed to focus to the left of center at $\lambda = \lambda_{\mathrm{Si}}$ with a plane wave incident from 0.5° to the right, and focus to the right of center at $\lambda = 1.001\lambda_{\mathrm{Si}}$ with a plane wave incident from 0.5° to the left, where λ here represents the wavelength in silicon at the actual frequency. Moment method and FDTD solutions for this structure at $\lambda = \lambda_{\mathrm{Si}}$ are shown in Fig. 32. They are in good agreement, but

differ from the results in Fig. 31. The reason for this difference has not yet been determined. The FDTD solution had the plane wave incident from directly above, and the frequency was the closest to $\lambda = \lambda_{\rm Si}$ that came out of the Fourier transform, but these small differences did not seem to make much difference. The moment method solution for this structure at $\lambda = 1.001\lambda_{\rm Si}$ is shown in Fig. 33 and is close to that for $\lambda = \lambda_{\rm Si}$.

The other dielectric pixel array in [1], Fig. 3 in that report, is for pixels of silicon in free space. The plots from [1] are reproduced here as Fig. 34. This design differs from the others in that the magnetic field H_z is parallel to the cylinders with E transverse. This case could not be modeled in the moment method without considerable additional effort. To model it we used the 2D FDTD code, solving for E_z, H_x and H_y, and applied duality. The pixels were modeled with $\mu_r = 12.1104$ with ϵ_0 and μ_0 interchanged, and E and H were interchanged for the plots. The result for $\lambda = \lambda_0$ is shown in Fig. 35. The reason for the disagreement with the results from [1] has not been determined.

Conclusion

Conducting strip arrays and conducting and dielectric pixel arrays designed by Webb and students at Purdue University to focus plane waves were modeled with moment method and FDTD codes. Some new designs were developed for the strip arrays using moment method modeling and the downhill simplex method of optimization with simulated annealing. Strip arrays in enclosures were also optimized as directional antennas. Some focusing of the antenna beam was demonstrated, although better results could be achieved by applying a little thought to the design before optimizing.

Webb and students used the iterative direct binary search method to optimize pixel arrays. We did not try optimizing these structures, but did model the Purdue designs with moment method and FDTD codes. Good agreement was obtained for the conducting pixel arrays. We could not reproduce the Purdue results for dielectric arrays.

References

[1] Kevin J. Webb, "Subwavelength Aperiodic Diffractive Elements," First Interim Report, Purdue University, 2004.

[2] Kevin J. Webb, " Sub-Wavelength Aperiodic Diffractive Elements," Interim Report, Purdue University, February 14, 2005.

[3] Webb and Li, private communication, February 4, 2005.

[4] W. H. Press, S. A. Teukolsky, W. T. Vetterling and B P. Flannery, *Numerical Recipes in Fortran* (also*Numerical Recipes in C*), Cambridge Univ. Press, New York, 1994.

[5] J. H. Richmond, "Scattering by a Dielectric Cylinder of Arbitrary Cross Section Shape," *IEEE Trans. Antennas and Propagation*, Vol. 13, No. 3, pp. 334-341, May 1965.

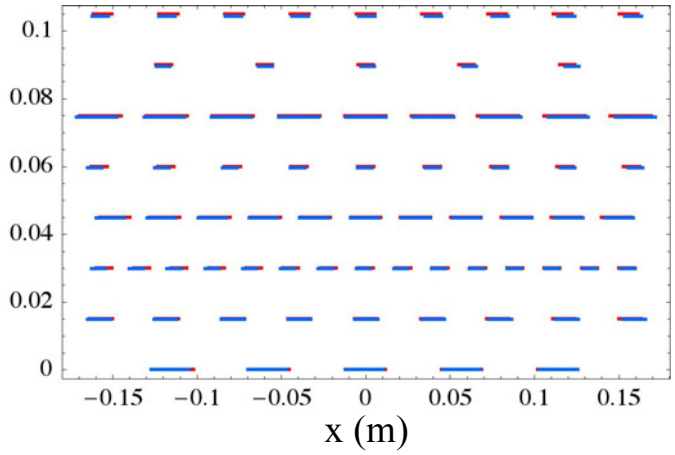

Fig. 1. Strip arrays for focusing a plane wave. The red lines were generated from parameters supplied by Webb and Li [3], and the blue lines were from parameters measured from the plot in Fig. 1 in [1].

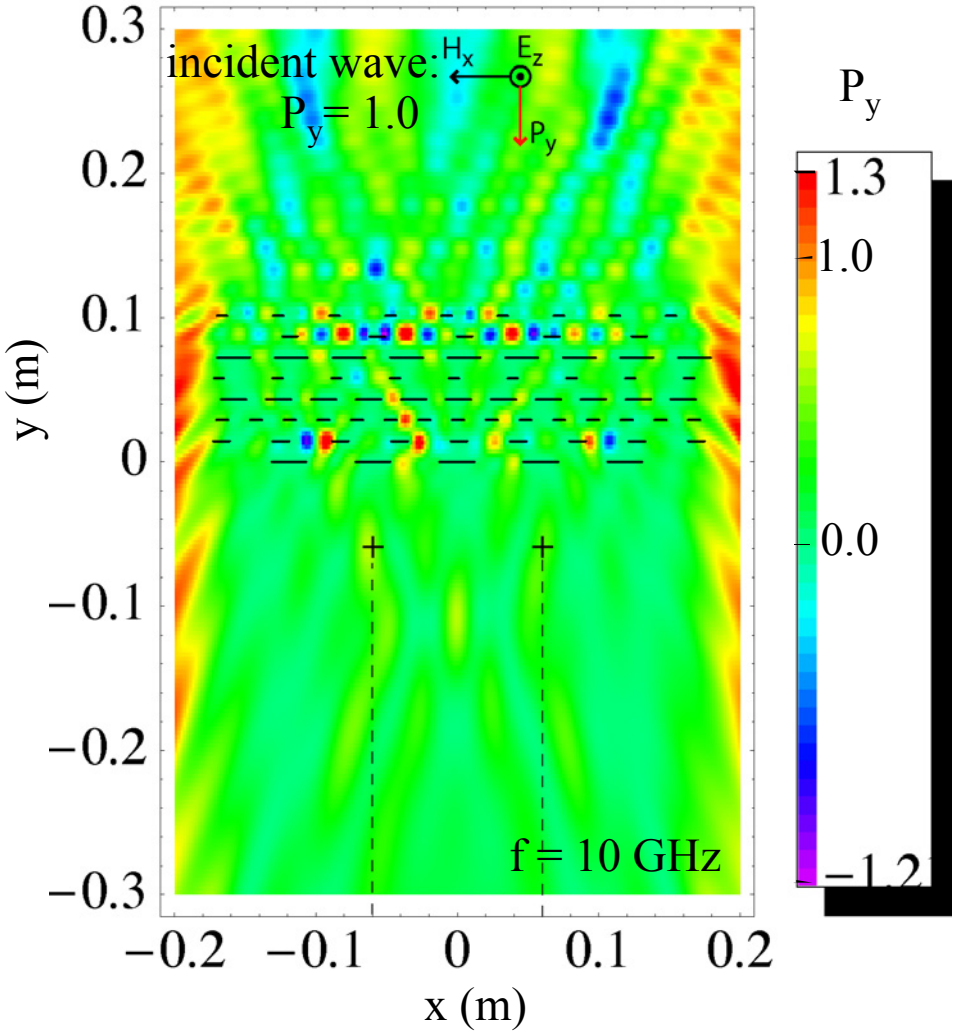

Fig. 2. Poynting's vector P_y (positive downward) for a plane wave passing through the strip array. Fields are from a moment method solution. The strip array is the blue lines in Fig. 1, measured from Fig. 1 in [1].

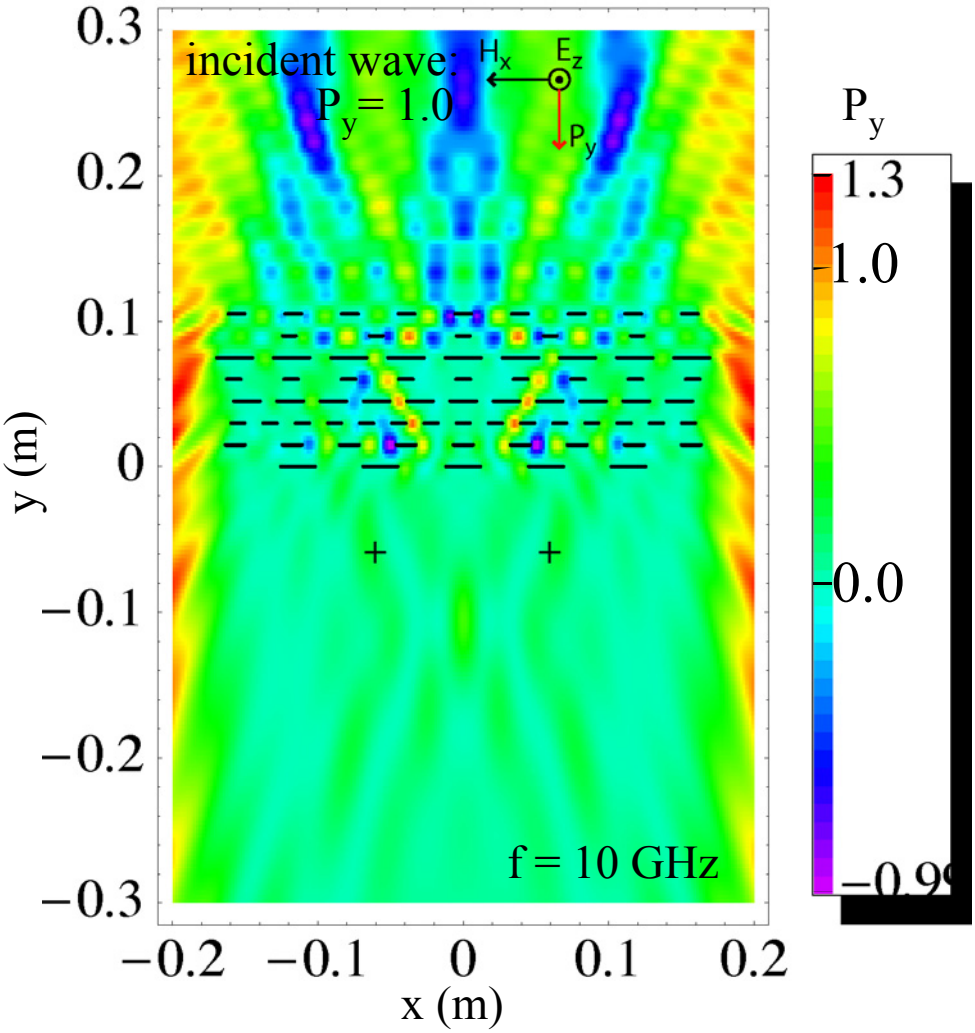

Fig. 3. Poynting's vector P_y (positive downward) from the moment method solution for a plane wave passing through the strip array with Webb's parameters from [3] (red lines in Fig. 1).

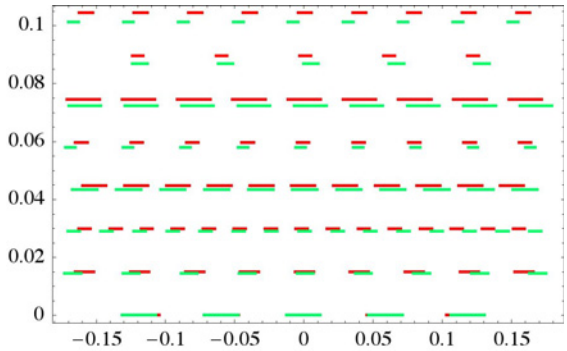

Fig. 4. Strip array measured from Fig. 1 in [1] (red) and the result of re-optimizing that array in the moment method solution (green).

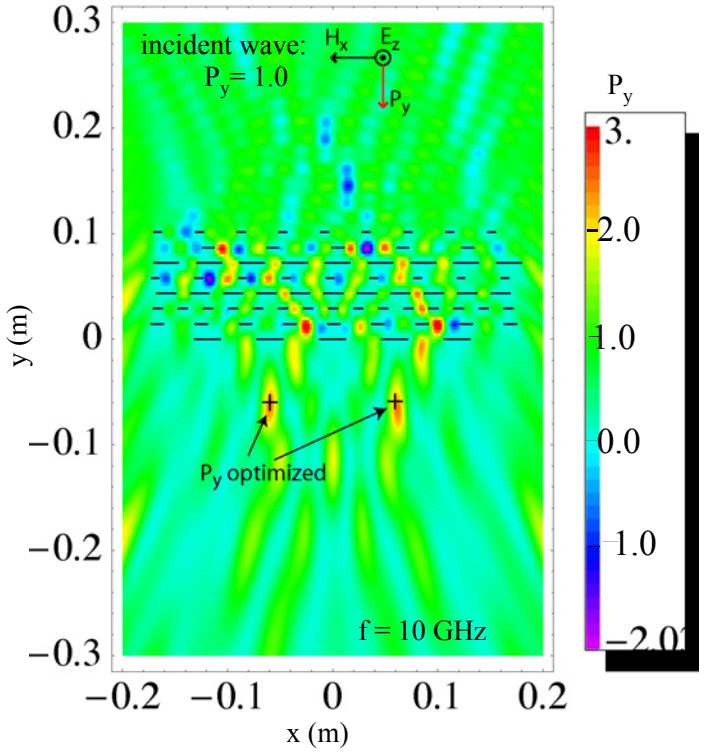

Fig. 5. Poyntings vector P_y (positive downward) that resulted from the re-optimized strip array (green) in Fig. 4.

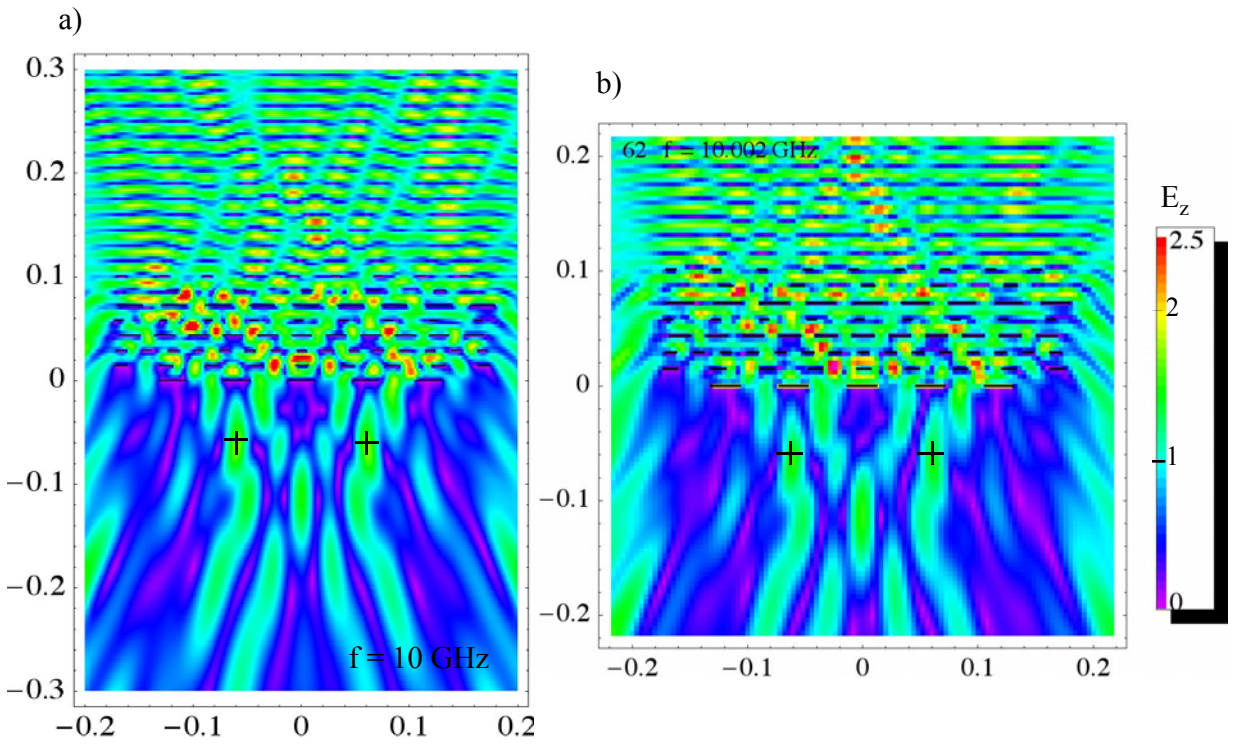

Fig. 6. E_z focused by the re-optimized strip array (green lines in Fig. 4). (a) moment method solution with $\Delta x = 0.0015$ m. (b) FDTD solution with $\Delta x = 0.0005$ m.

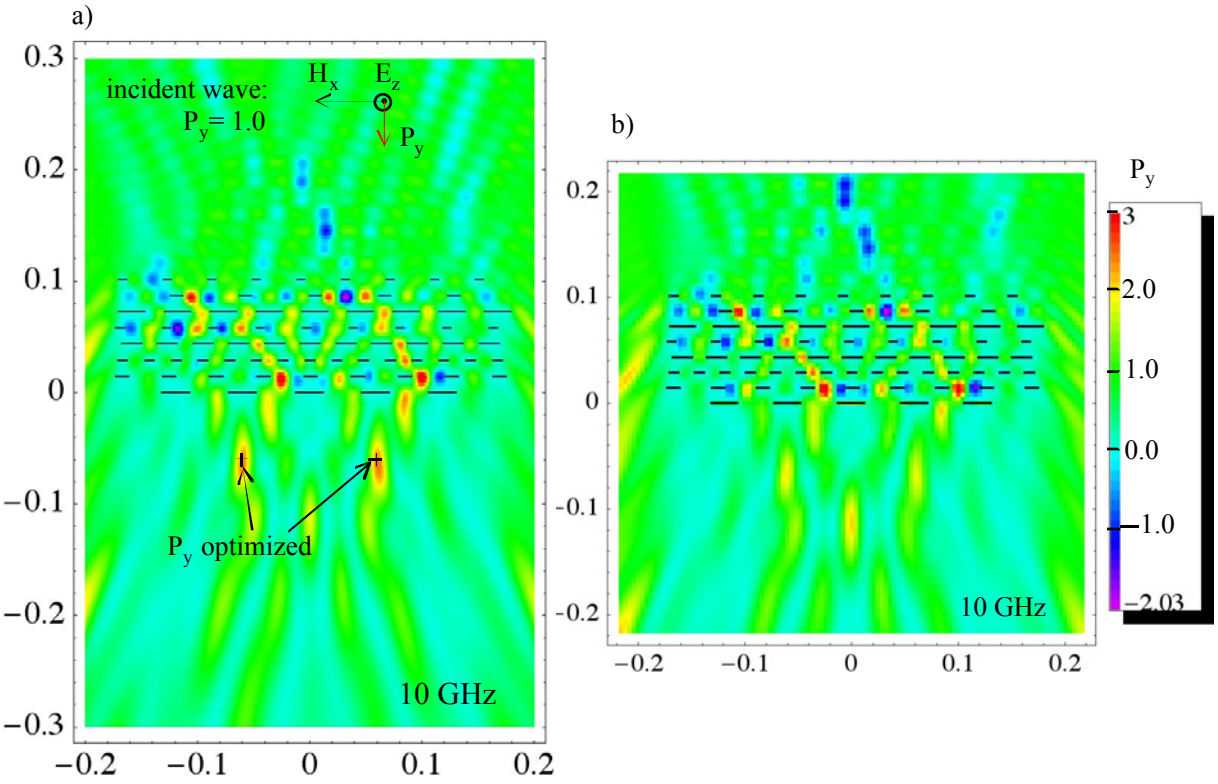

Fig. 7. Poynting's vector P_y focused by the re-optimized strip array (green lines in Fig. 4). (a) moment method solution. (b) FDTD solution.

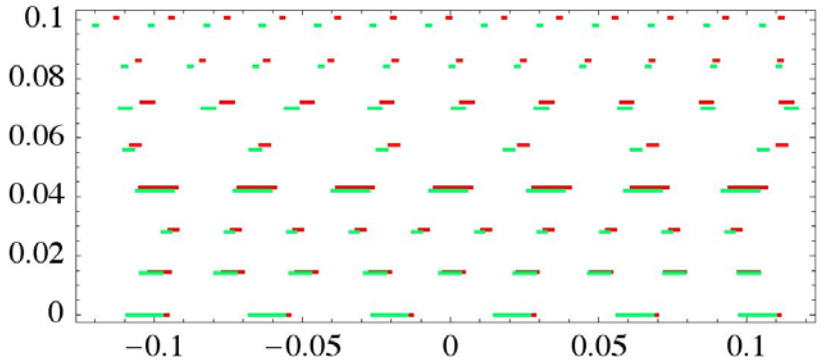

Fig. 8. Strip array optimized to focus a plane wave at $x = -0.06$ and $+0.06$ m for $y = -0.06$ m. The red lines were obtained after the initial optimization and the green after further optimization with simulated annealing.

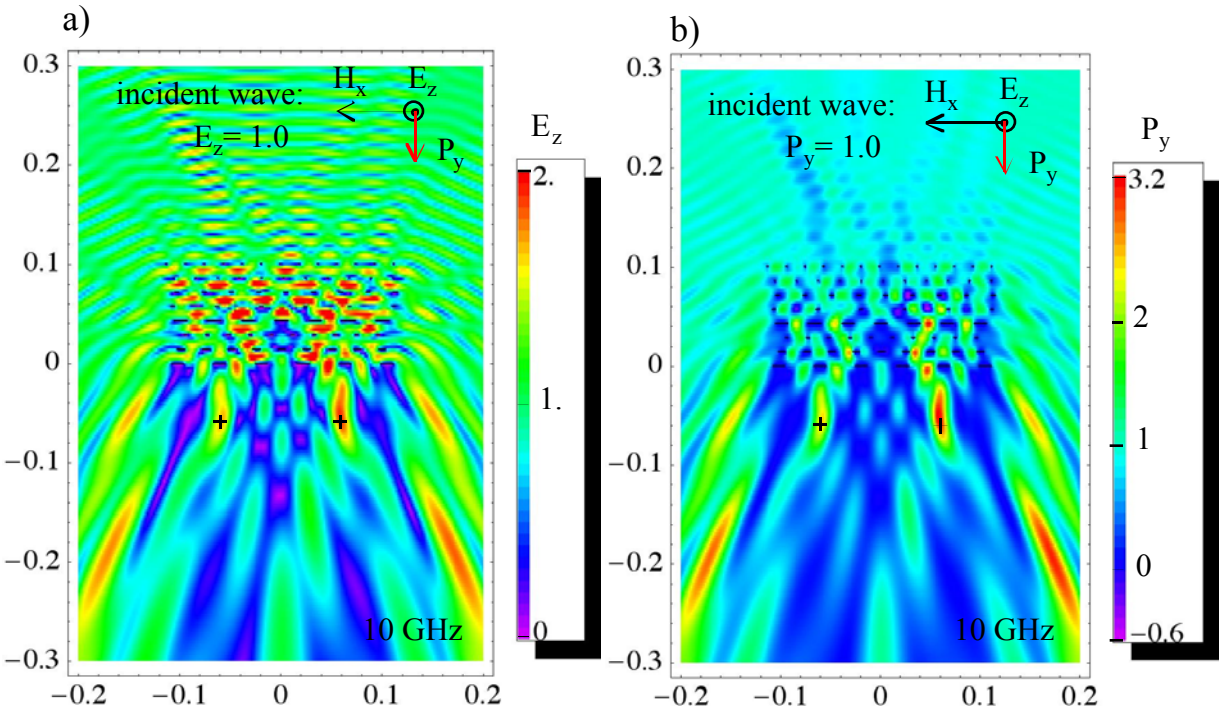

Fig. 9. E_z (a) and Poynting's vector P_y (b), positive downward, for the red strip array in Fig. 8.

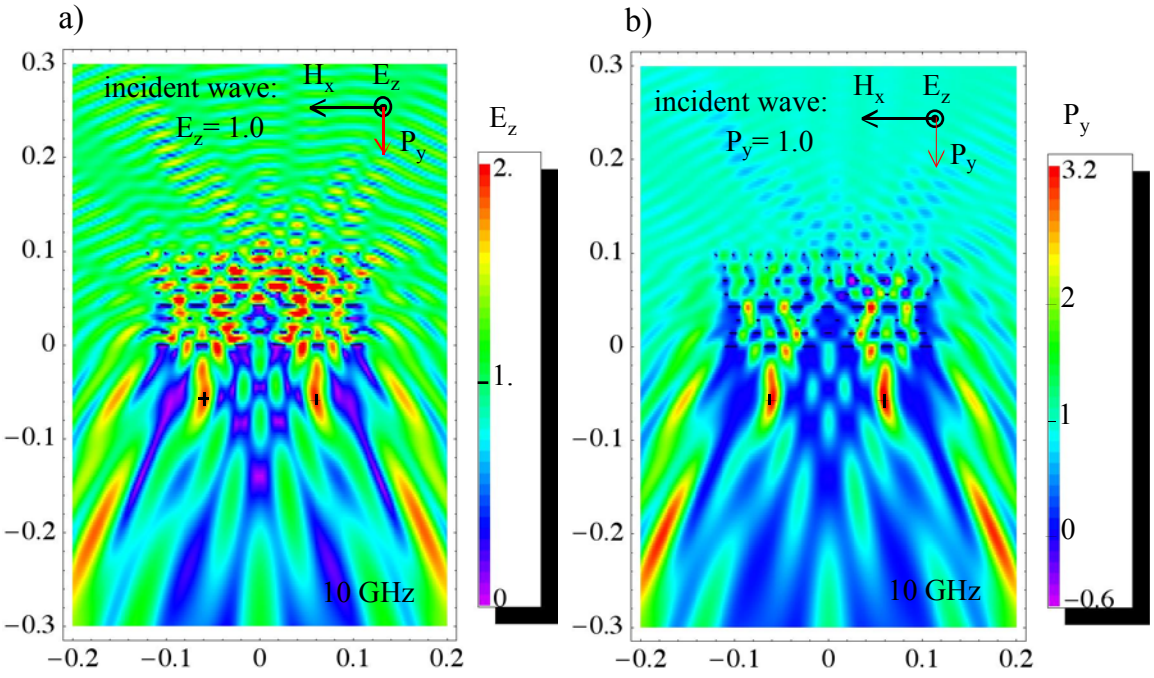

Fig. 10. E_z (a) and Poynting's vector P_y (b), positive downward, for the green strip array in Fig. 8.

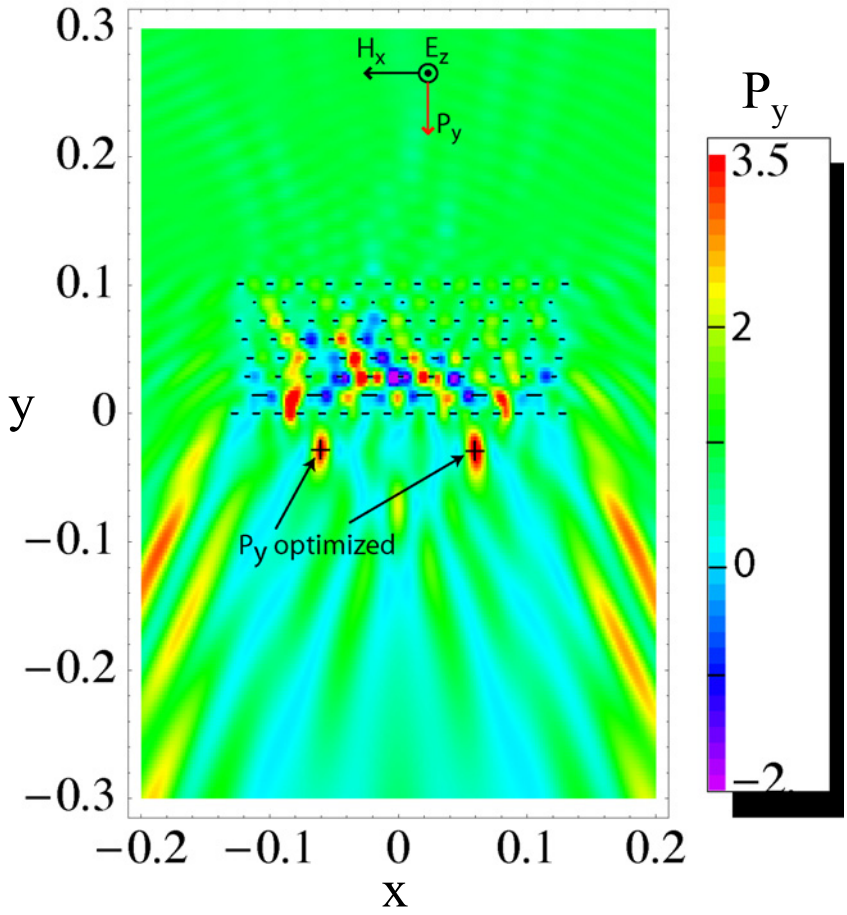

Fig. 11. Poynting's vector P_y for a strip array optimized to focus a plane wave at $x = -0.06$ m and 0.06 m for $y = -0.03$ m.

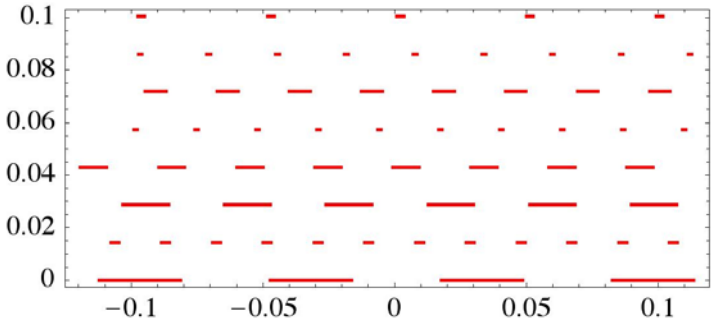

Fig. 12. E_z (a) and Poynting's vector P_y (b), positive downward, for the green strip array in Fig. 8.

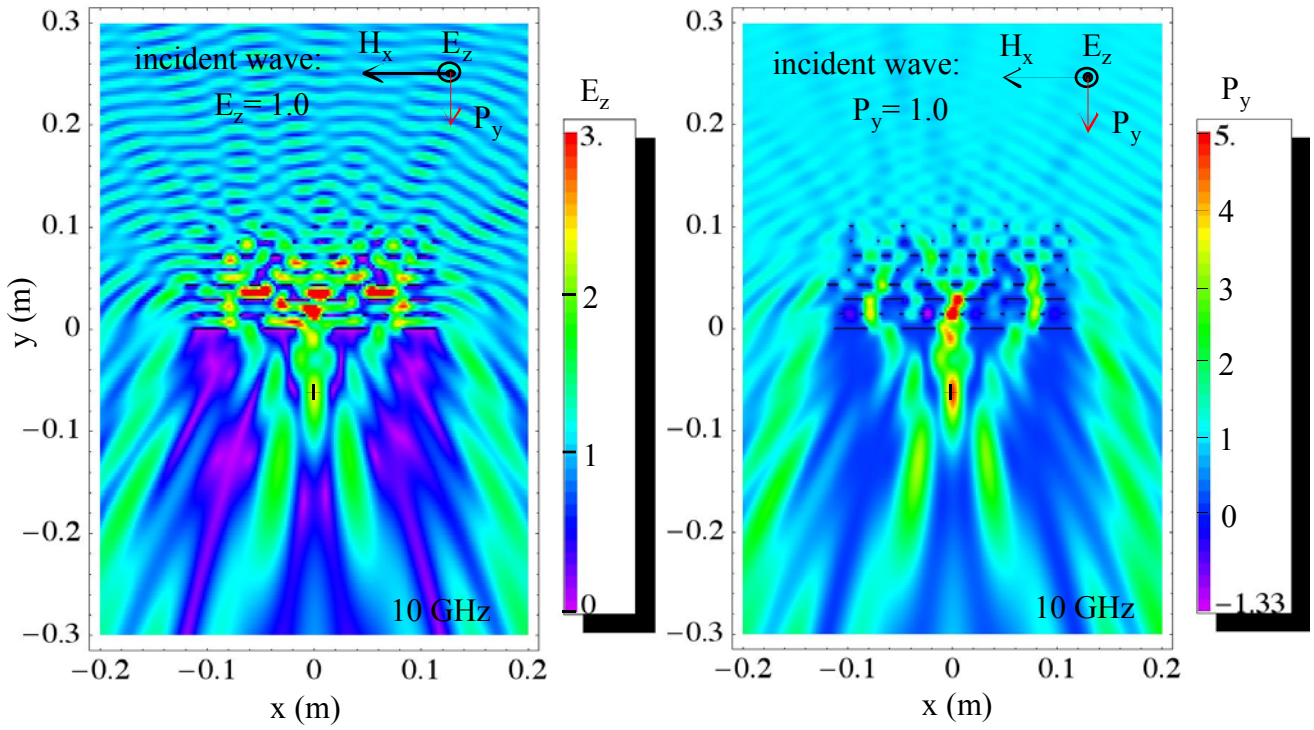

Fig. 13. Poynting's vector P_y (positive downward) for the strip array in Fig. 12.

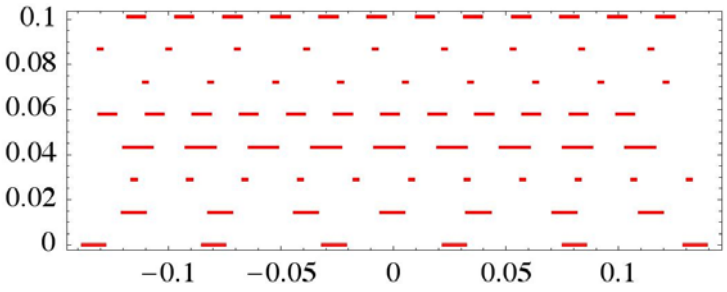

Fig. 14. Strip array optimized to focus a plane wave at $x = -0.06$ m at 9.5 GHz and $x = +0.06$ m at 10 GHz for $y = -0.06$ m.

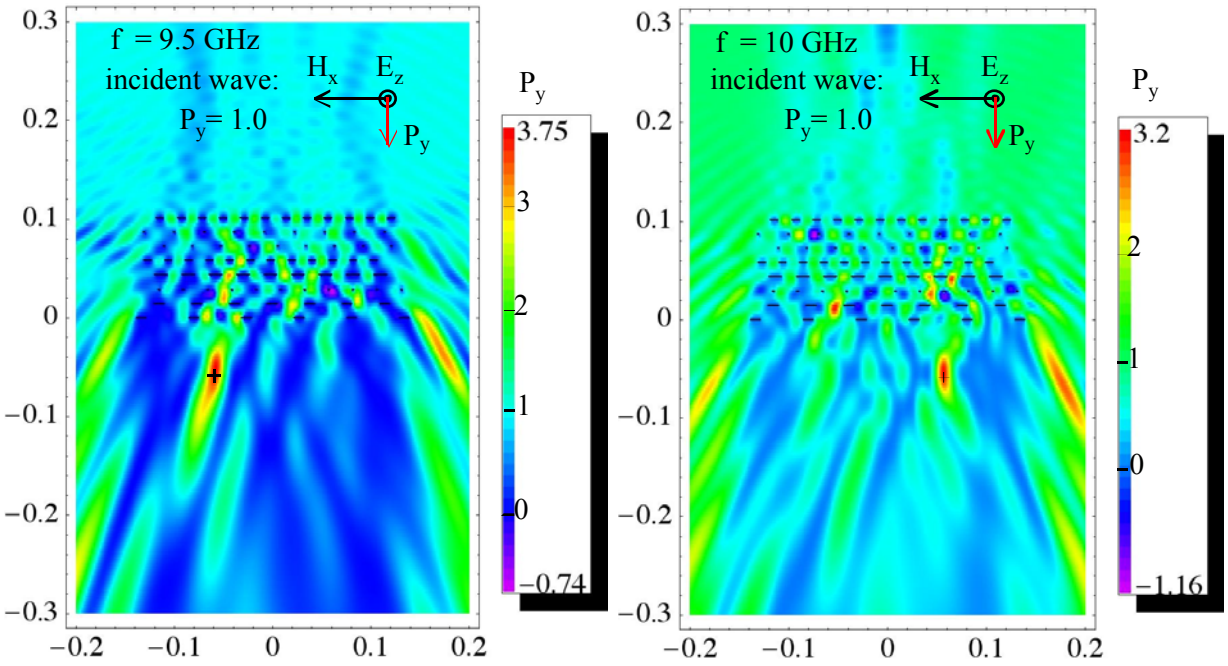

Fig. 15. Poynting's vector P_y (positive downward) for the strip array in Fig. 14, focusing at $x = -0.06$ m at 9.5 GHz and at $x = 0.06$ m at 10 GHz.

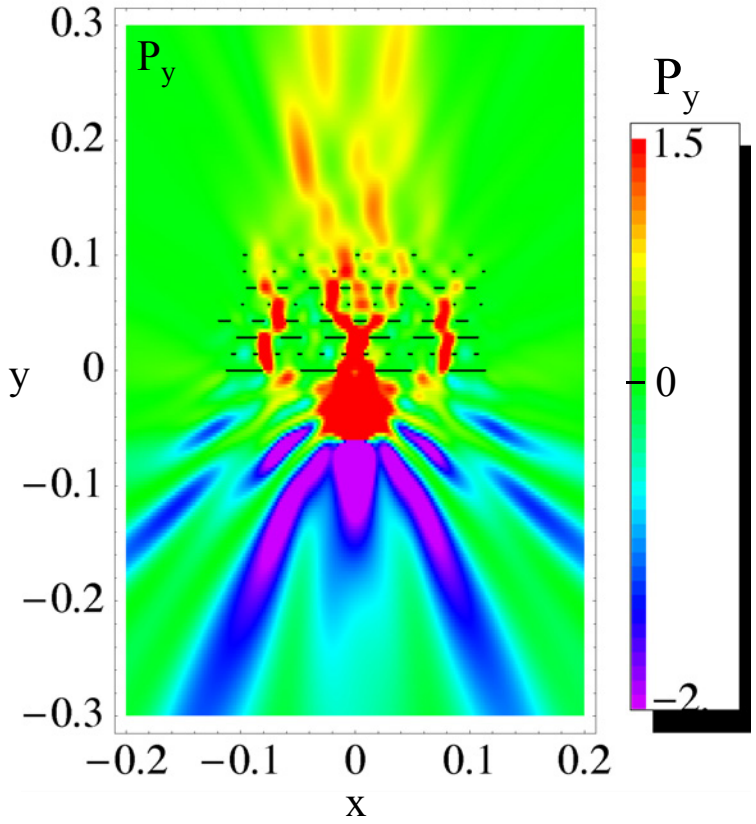

Fig. 16. Poynting's vector P_y (positive upward) for the strip array in Fig. 12 with a line current source at the focus point $x = 0$, $y = -0.06$ m at 10 GHz.

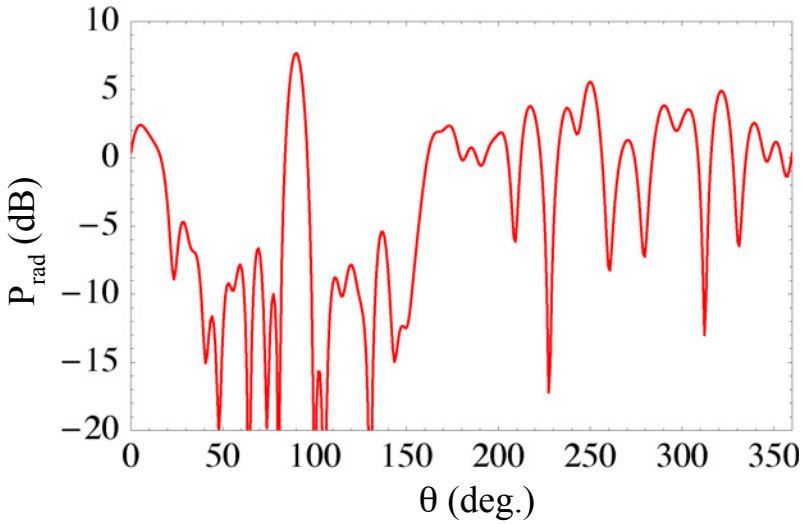

Fig. 17. Far field radiation pattern for the strip array in Fig. 12 with a line current source at the focus point $x = 0$, $y = -0.06$ m at 10 GHz.

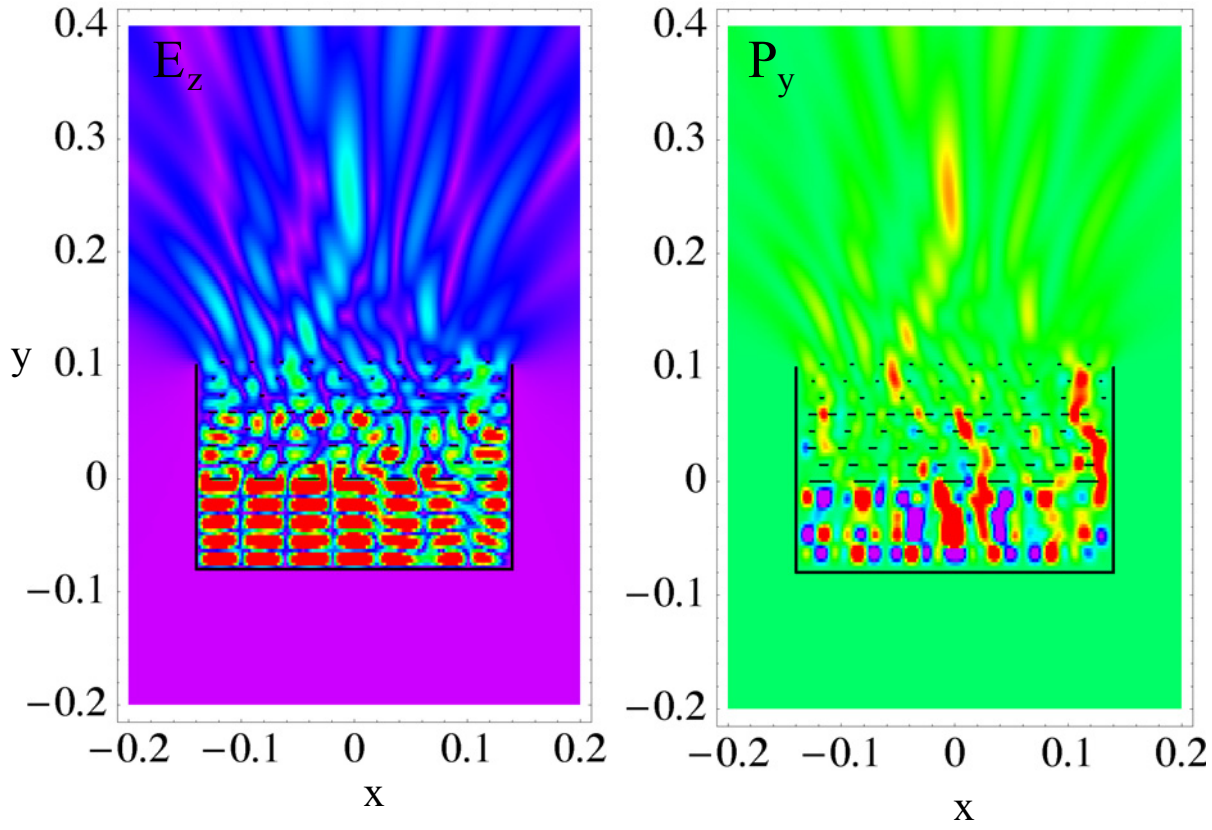

Fig. 18. Electric Field E_z and Poynting's vector P_y for a strip array in a box with a line current source at $x = 0$, $y = -0.06$ m. The strip array was optimized to focus an incident plane wave at the source location at 10 GHz.

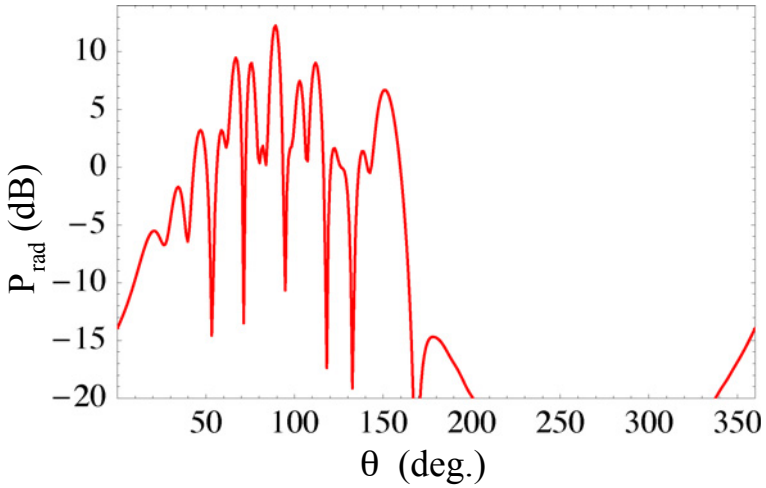

Fig. 19. Far field radiation pattern for the strip array in Fig. 18 with a line current source at the focus point $x = 0$, $y = -0.06$ m at 10 GHz.

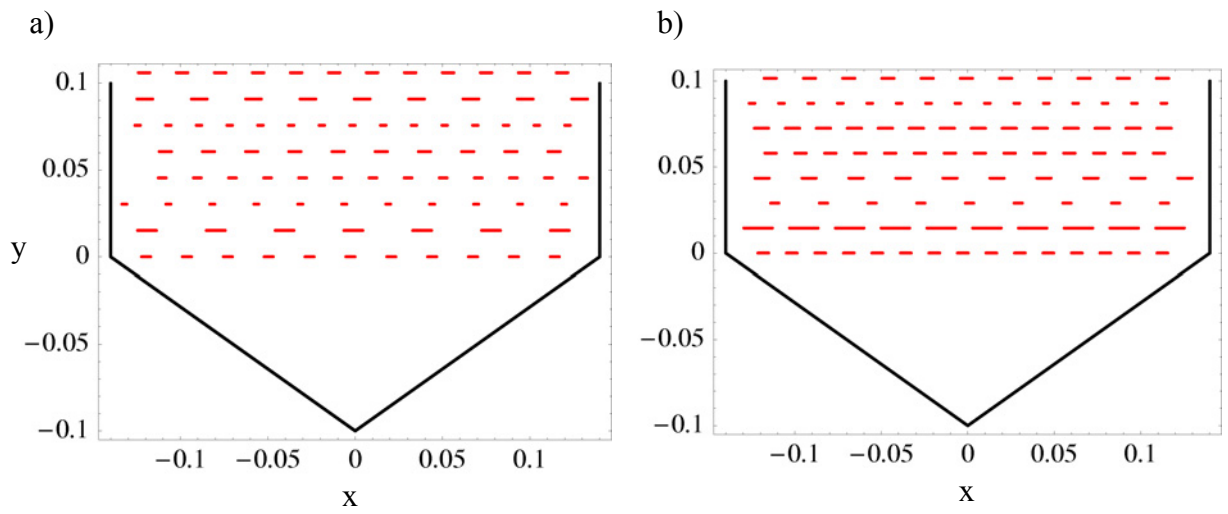

Fig. 20. Strip arrays in a box with angled bottom. (a) Strips optimized to focus an incident plane wave at $x = 0$, $y = -.06$ m. (b) Strips optimized for an upward beam with a line source at $x = 0$, $y = -.06$ m.

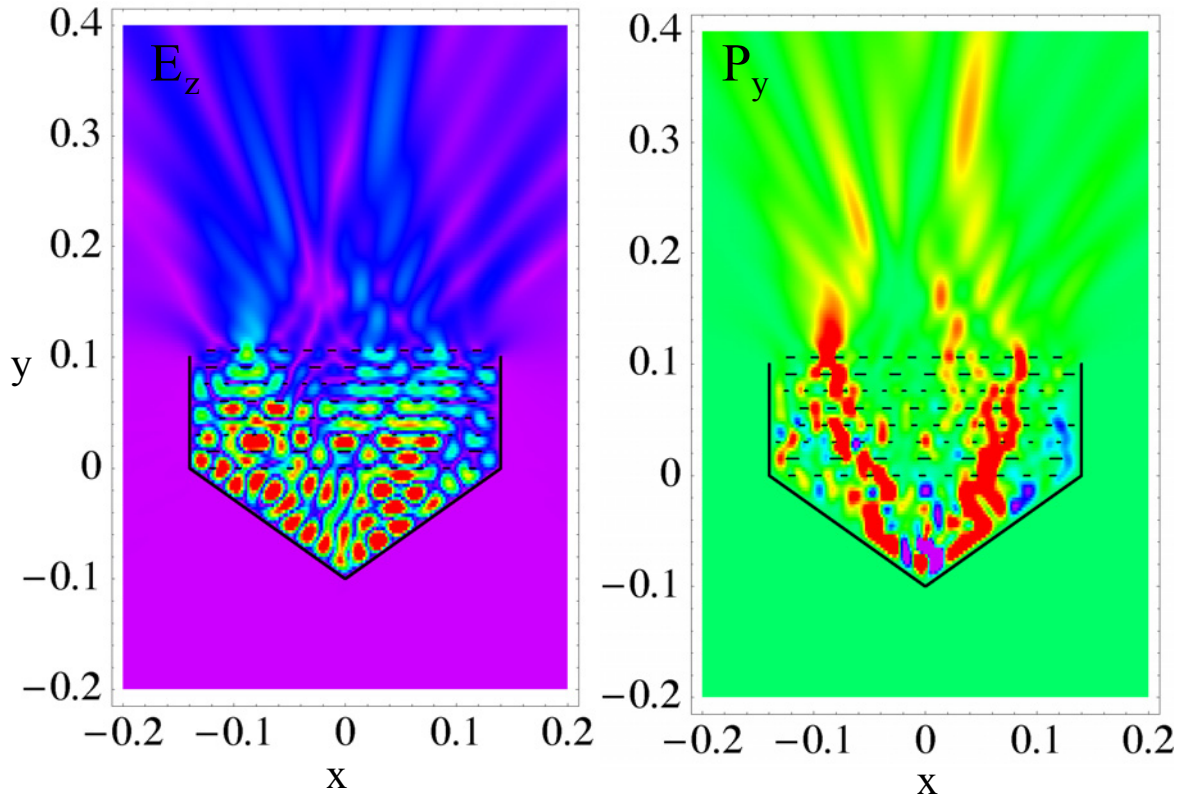

Fig. 21. Electric Field E_z and Poynting's vector P_y for the strip array in Fig. 20(a) at 10 GHz.

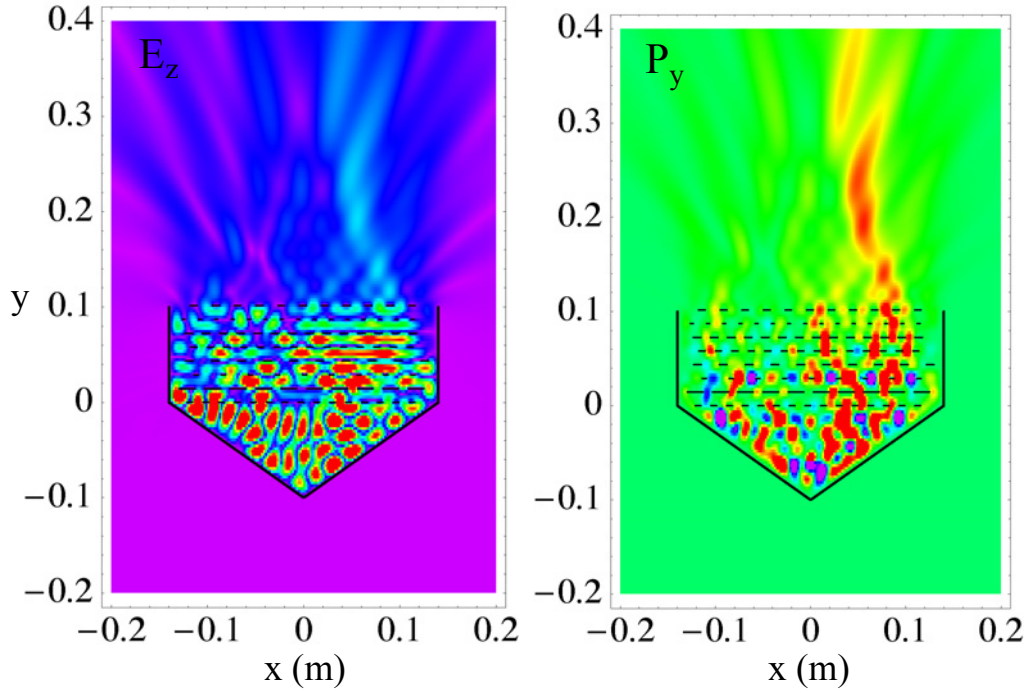

Fig. 22. Electric Field E_z and Poynting's vector P_y for the strip array in Fig. 20(b) at 10 GHz.

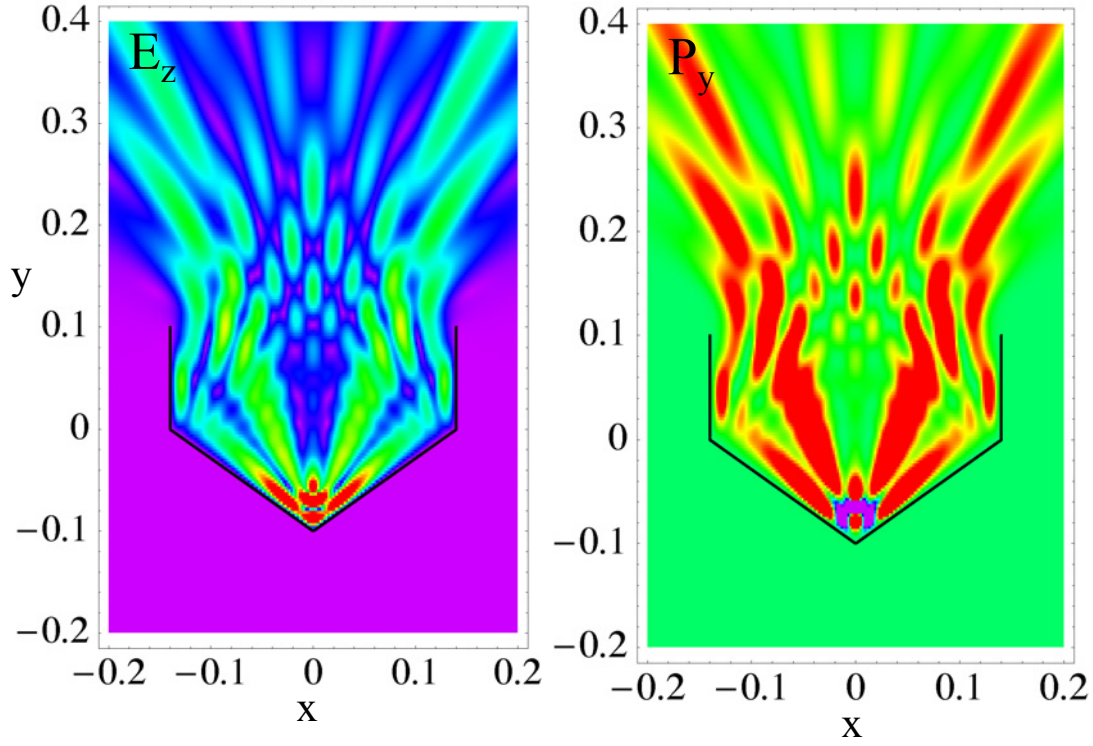

Fig. 23. Electric Field E_z and Poynting's vector P_y for a line current source at $x = 0$, $y = -0.06$ m in the box of Fig. 20 without the strip array.

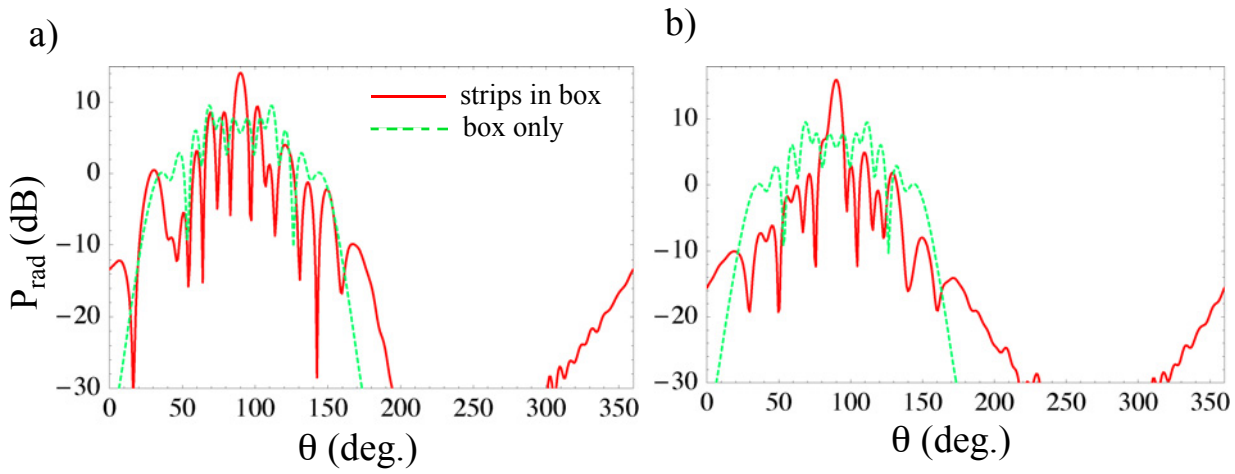

Fig. 24. Far field radiation patterns for strip arrays in Fig. 20 with a line current source at the focus point $x = 0$, $y = -0.06$ m at 10 GHz. (a) Strip array from Fig. 19(a). (b) Strip array from Fig. 20(b). The pattern for the source in the box without strip array is included for comparison.

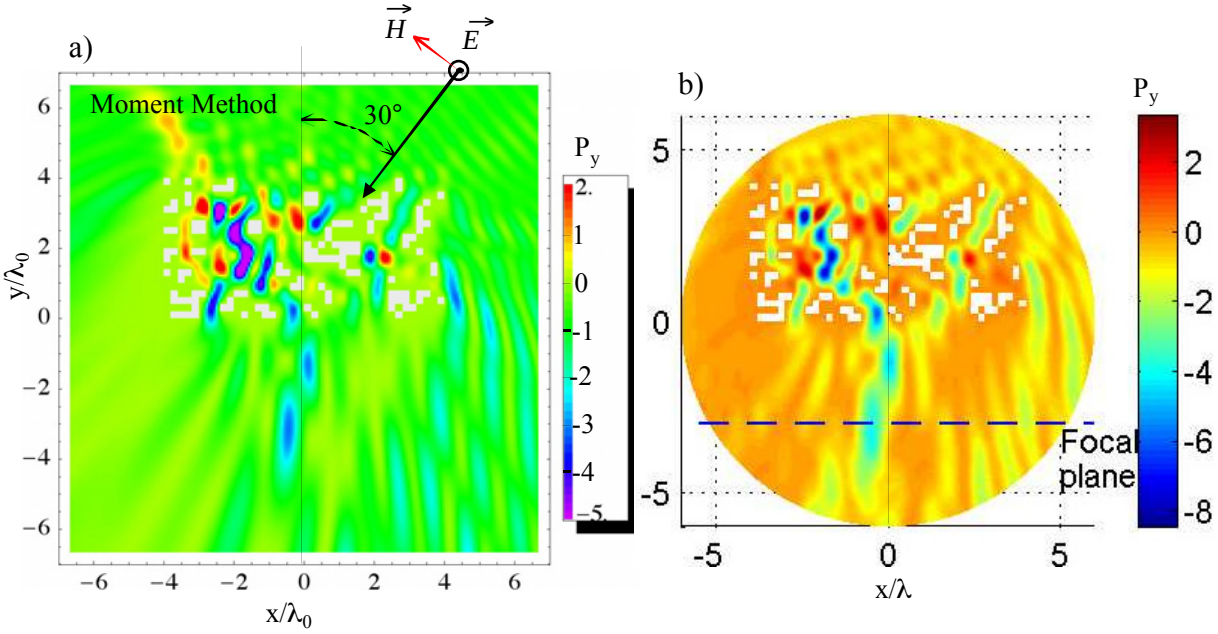

Fig. 25. P_y focused by an array of conducting pixels optimized by Webb and Li [1]. The results are for a frequency $\lambda = \lambda_0$ where it was designed to focus to the left of center. (a) Moment method solution. (b) Webb and Li's finite element solution (figure taken from [1].)

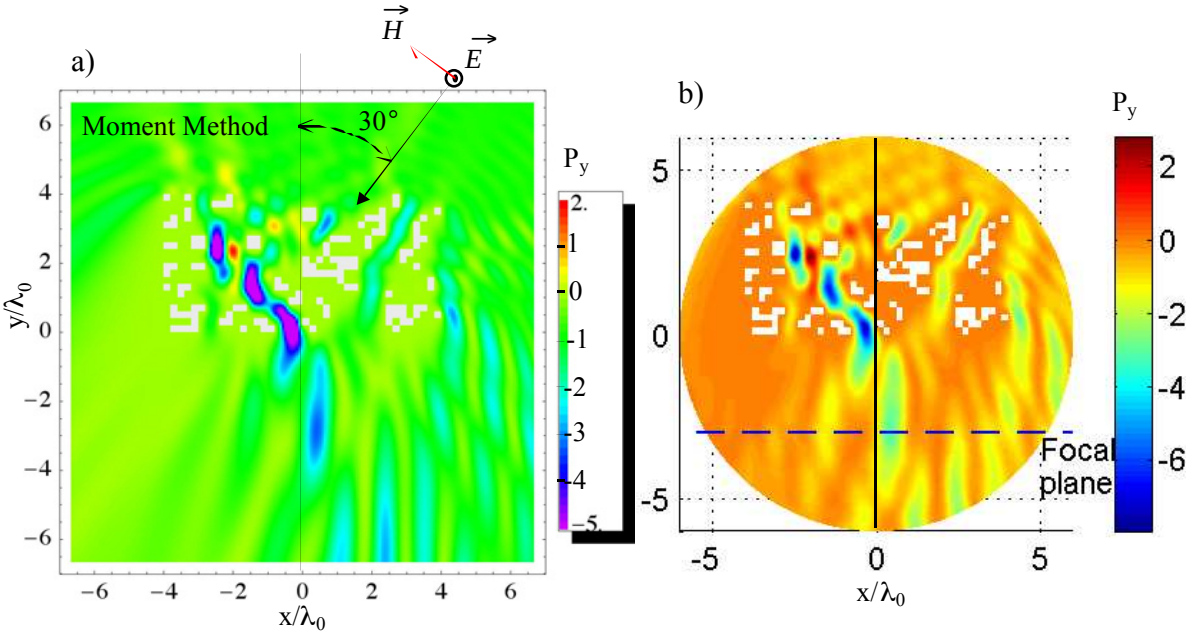

Fig. 26. P_y focused by an array of conducting pixels optimized by Webb and Li [1]. The results are for a frequency $\lambda = 1.1\lambda_0$ where it was designed to focus to the right of center. (a) Moment method solution. (b) Webb and Li's finite element solution (figure taken from [1].)

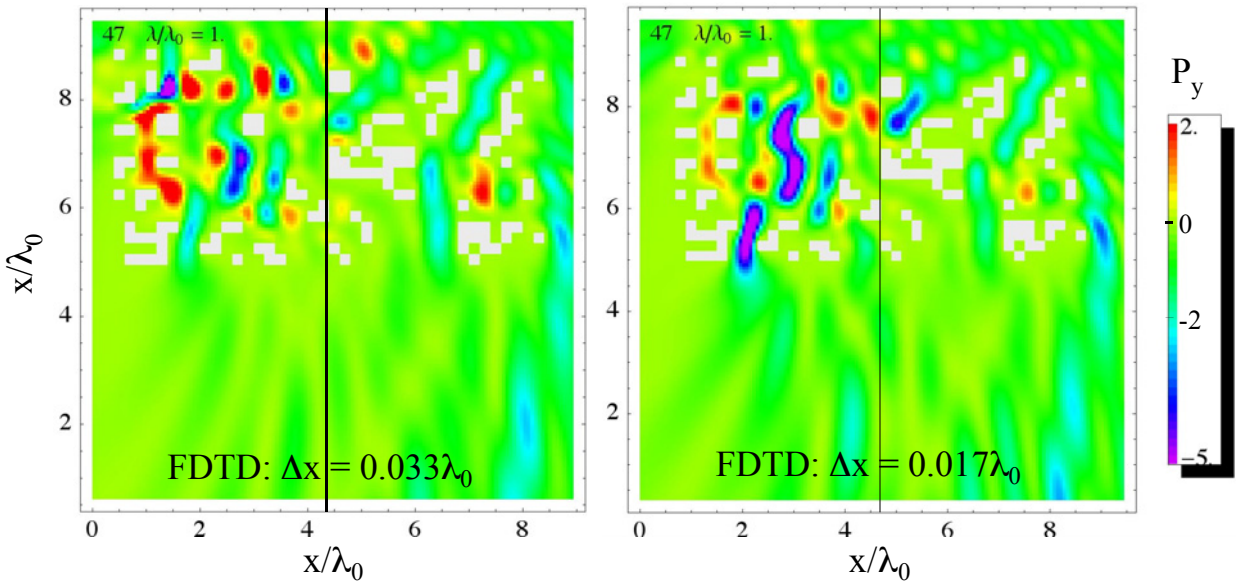

Fig. 27. Array of conducting pixels optimized by Webb and Li [1] modeled by the FDTD method for frequency $\lambda = \lambda_0$. The results for FDTD mesh resolution of $0.033\lambda_0$ and $0.017\lambda_0$ are converging toward the moment method and FE solutions in Fig. 25.

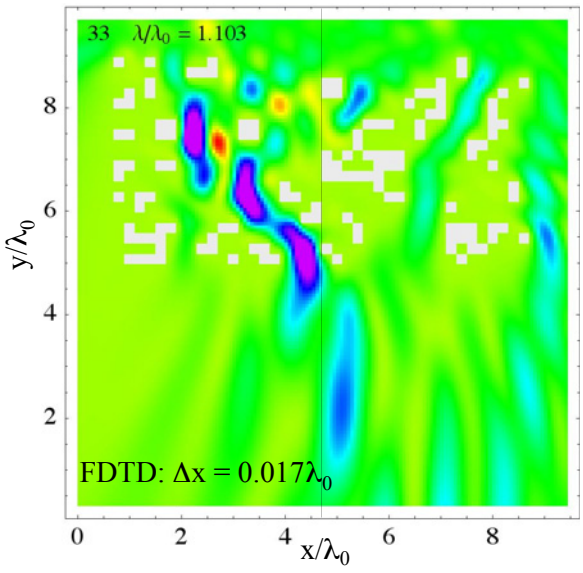

Fig. 28. Array of conducting pixels optimized by Webb and Li [1] modeled by the FDTD method for frequency $\lambda = 1.103\lambda_0$. The result agrees with the moment method and finite element solutions in Fig. 26.

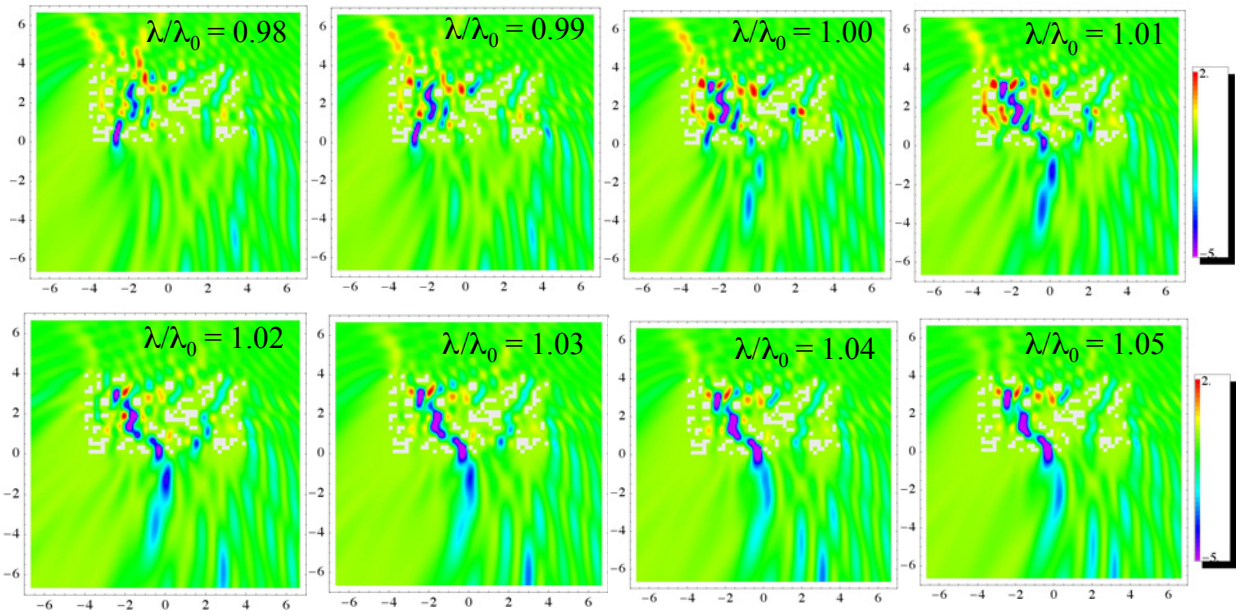

Fig. 29. P_y for a plane wave incident on the array of conducting pixels optimized by Webb and Li [1] for frequencies of $\lambda/\lambda_0 = 0.98$ to 1.05 from the moment method solution.

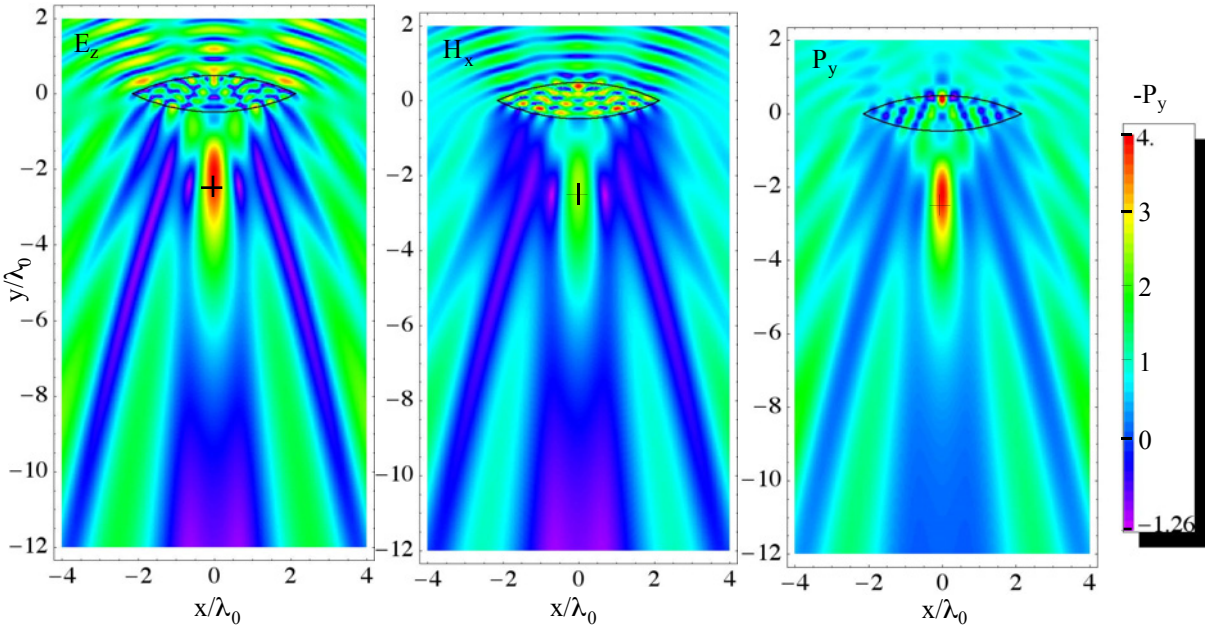

Fig. 30. Dielectric lens with $\epsilon_r = 4$ and cylinder axis along z modeled by the moment method. Plots show E_z, H_x and the y component of Poynting's vector P_y (positive downward) for a plane wave incident from above.

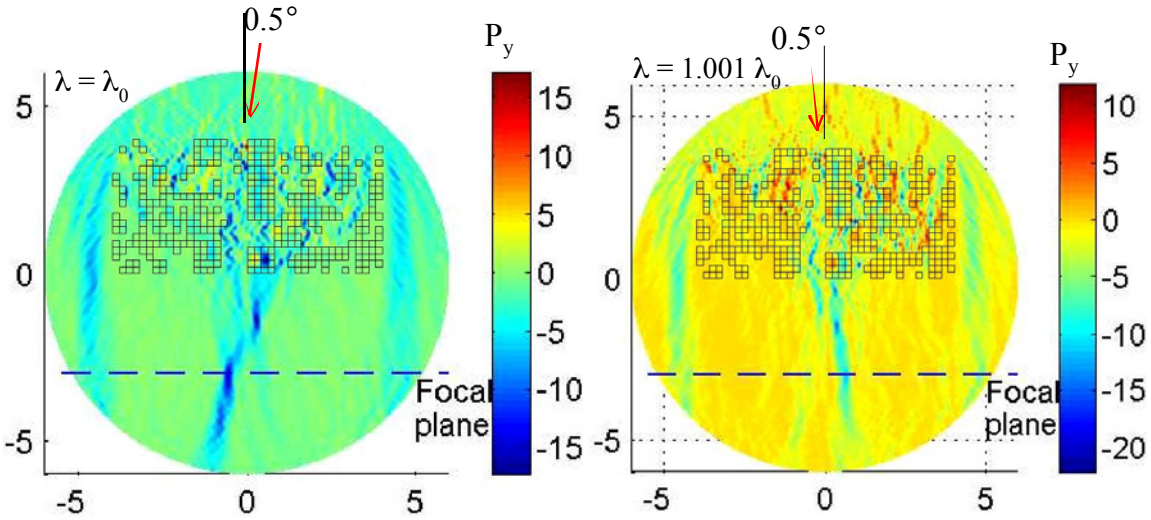

Fig. 31. Array of dielectric pixels with $\epsilon_r = 2.0852$ in a background medium of $\epsilon_r = 12.1104$ optimized by Webb and Li [1]. The array is designed to focus to the left with a plane wave incident from 0.5° to the right at $\lambda = \lambda_0$, and focus to the right with a plane wave incident from 0.5° to the left at $\lambda = 1.001\lambda_0$.

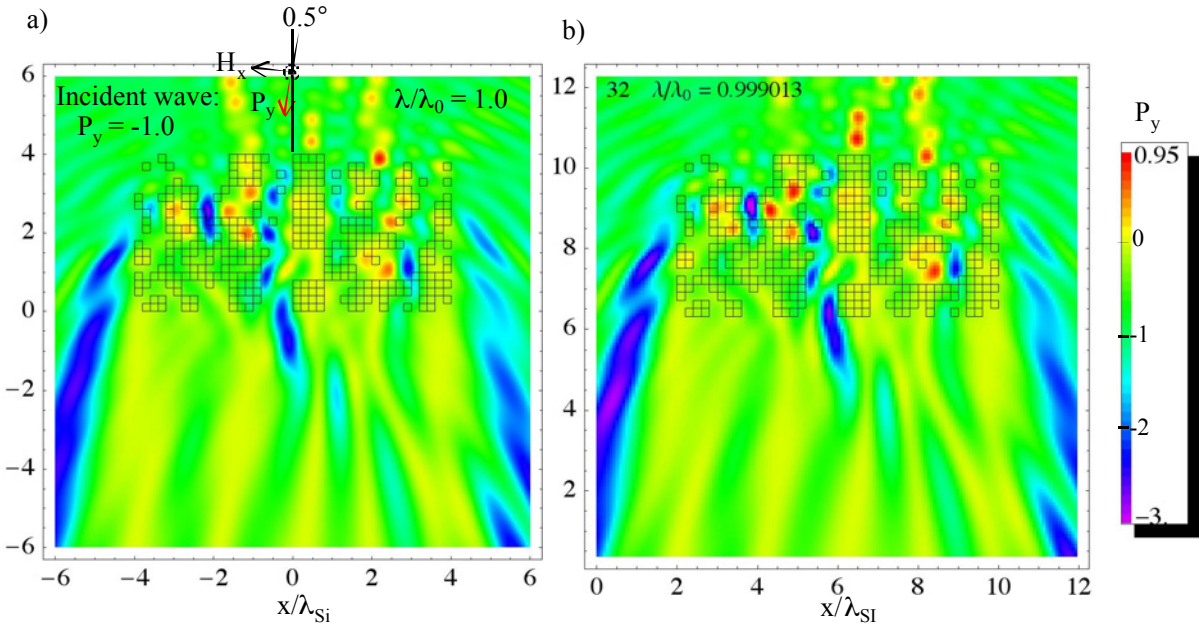

Fig. 32. Array of dielectric pixels from Fig. 31 with $\epsilon_r = 2.0852$ in a background medium of $\epsilon_r = 12.1104$ optimized by Webb and Li [1]. (a) Moment method solution for the downward Poynting's vector for a plane wave incident from 0.5° to the right at $\lambda = \lambda_0$. (b) FDTD solution for a plane wave incident from directly above with $\lambda = 0.999013\lambda_0$.

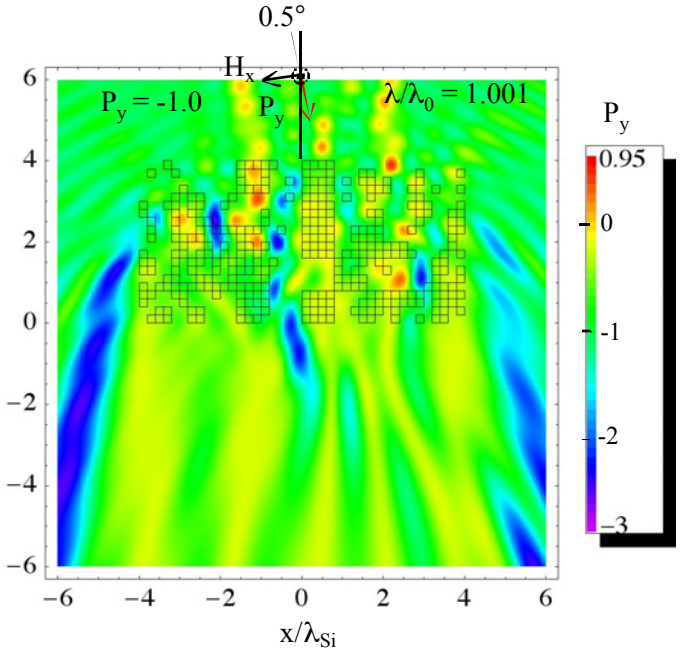

Fig. 33. The same structure as Fig. 32 for a plane wave incident from 0.5° to the left at $\lambda = 1.001\lambda_0$ from a moment method solution.

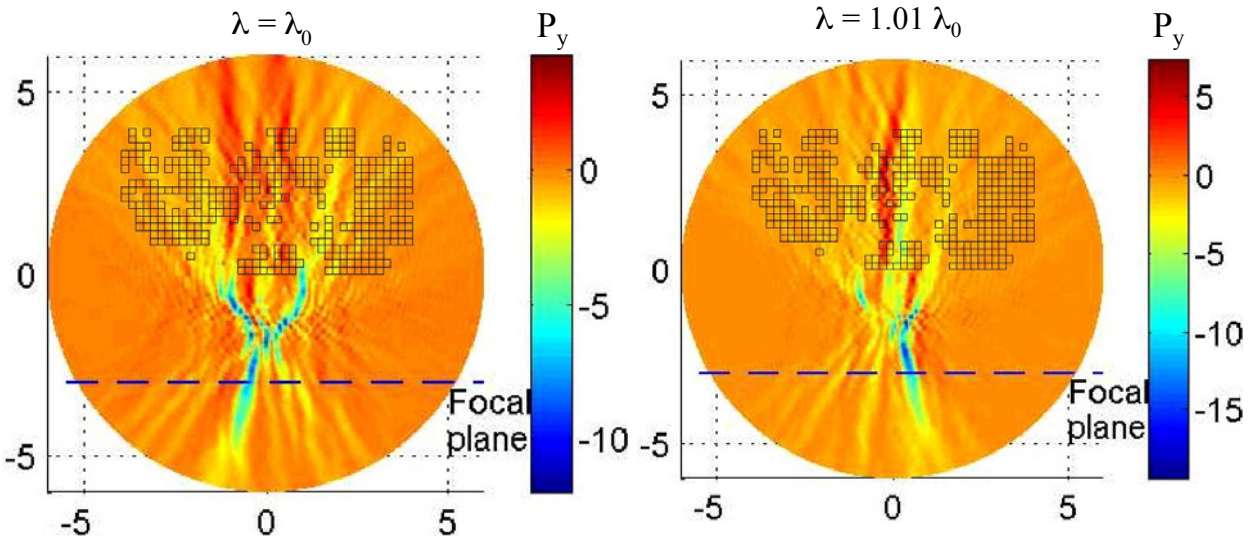

Fig. 34. Array of dielectric pixels with $\epsilon_r = 12.1104$ in a background medium of free space optimized by Webb and Li [1]. The plane wave is incident from above with H_z parallel to the cell axis. The array is designed to focus to the left at $\lambda = \lambda_0$, and focus to the right at $\lambda = 1.01\lambda_0$. The figures are from [1].

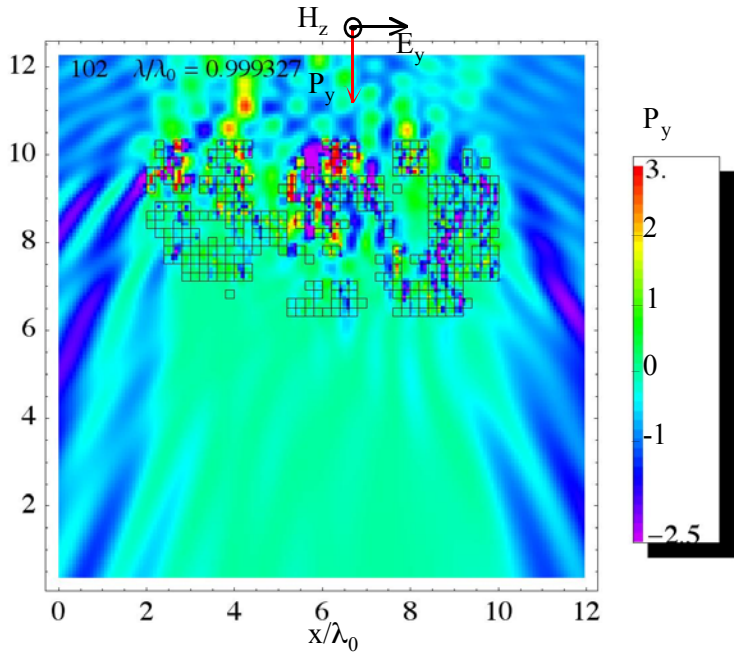

Fig. 35. FDTD solution for the dielectric pixel array in Fig. 34 for $\lambda = 0.999327\lambda_0$ from a FDTD solution.